Tremor and Other Hyperkinetic Movements

Thalamic and Visual Network Dysfunction Relates to Tremor Response in Thalamic Deep Brain Stimulation

ARTICLE

AIMEE E. MORRIS
BABATUNDE ADEYEMO
MEGHAN C. CAMPBELL
ABRAHAM Z. SNYDER
JOEL S. PERLMUTTER
JONATHAN W. MINK
SCOTT A. NORRIS

*Author affiliations can be found in the back matter of this article

ubiquity press

ABSTRACT

Background: Essential tremor (ET) is the most common movement disorder in adults, but its pathogenesis is incompletely understood. Deep brain stimulation of the ventral intermediate thalamic nucleus (VIM DBS) provides effective treatment for medically-refractory cases. We aimed to determine how pre-surgical resting-state functional connectivity (FC) in medically-refractory ET relates to VIM DBS clinical response.

Methods: We analyzed resting-state FC MRI in 21 participants with medically-refractory ET who subsequently underwent VIM DBS and 34 matched controls. We applied rigorous quality assurance to minimize motion artifact. Whole-brain correlation matrices were computed across 300 cortical, subcortical, and cerebellar regions and compared across groups using object-oriented data analysis, a powerful novel approach. We used multiple linear regression to determine whether network FC (calculated as mean cross-correlation between nodes) in defined networks predicts VIM DBS response. We assessed regional FC using a seed in motor thalamus.

Results: Whole-brain correlation matrices and regional motor thalamus FC differed significantly between groups. Post-hoc network-level testing revealed decreased thalamus-somatomotor, thalamus-visual, and auditory-visual FC in ET versus controls. Regional FC showed increased primary motor cortex and decreased occipital-parietal and cerebellar FC with motor thalamus in ET relative to controls. Visual-lateral somatomotor network FC negatively predicted tremor improvement with VIM DBS.

Discussion: Whole-brain, network, and regional FC results demonstrate cerebello-thalamo-motor pathway dysfunction in ET. Robust FC differences in motor and visual regions related to VIM DBS outcomes. These results, employing rigorous quality control, support the need for additional investigation into the role of visual cortical networks in ET and DBS response.

CORRESPONDING AUTHOR:
Scott A. Norris, M.D.
Campus Box 8111, Washington University School of Medicine, 660 South Euclid Avenue, St. Louis, Missouri, 63110, USA
norriss@wustl.edu

KEYWORDS:
Essential tremor; functional connectivity; resting-state fMRI

TO CITE THIS ARTICLE:
Morris AE, Adeyemo B, Campbell MC, Snyder AZ, Perlmutter JS, Mink JW, Norris SA. Thalamic and Visual Network Dysfunction Relates to Tremor Response in Thalamic Deep Brain Stimulation. *Tremor and Other Hyperkinetic Movements.* 2025; 15(1): 34, pp. 1–15. DOI: https://doi.org/10.5334/tohm.1039

INTRODUCTION

Essential tremor (ET) is characterized by isolated bilateral upper limb action tremor of at least three years duration, with or without tremor in other body regions, and absence of other neurological signs [1]. Although ET is the most common movement disorder, the underlying pathophysiologic network mechanisms relating to effective therapeutic intervention, including deep brain stimulation (DBS) are incompletely understood.

Multiple studies have implicated dysfunction in the cerebello-thalamo-cortical network in the pathogenesis of ET, on the basis of electrophysiologic [2], functional neuroimaging [3–7], and neuropathology [8–10] data. Despite our growing knowledge, the precise relations between these identified abnormalities, symptomatology, and treatment response in ET remains poorly understood. Neuroimaging may reveal previously unrecognized brain regions or networks that play a key role in ET pathophysiology or its treatment. In particular, neuroimaging provides a comprehensive and simultaneous examination of the whole brain, facilitating the identification of relevant abnormalities. Indeed, prior functional neuroimaging studies have identified abnormalities in various brain regions outside of the cerebello-thalamo-cortical circuit, including visual cortex [11, 12], middle temporal cortex [13], and inferior parietal cortex [7]. However, neuroimaging findings in ET outside of the cerebello-thalamo-cortical motor network have been inconsistent.

Resting-state functional connectivity magnetic resonance imaging (rs-fMRI) is a powerful method to study network-level dysfunction that can avoid confounds of interpretation from differences in motor performance or abnormal movements during task-based MRI studies [14].

VIM DBS effectively reduces tremor in patients with medically refractory ET [14]. Positron emission topography neuroimaging has shown that clinically effective VIM DBS produces a robust blood flow response to stimulation in the ventral thalamus and ipsilateral supplementary motor area (SMA), a cortical target of VIM efferents [15]. Prior work has shown that strong structural and functional connectivity between thalamic DBS stimulation sites and primary sensorimotor cortex, SMA, and cerebellum correlates with improved tremor suppression [16, 17]. Outside of the cerebello-thalamo-cortical network, thalamo-visual-motor FC has been identified as a potential preoperative predictor of tremor arrest after VIM thalamotomy [18–20]. Seed regions derived from VIM DBS stimulation sites in patients with ET applied to large normative datasets have identified thalamic structural and functional connectivity with V1 and V2 (in addition to S1, M1, cerebellum, and superior temporal gyrus) as potential predictors of thalamic DBS response [21]. However, this observation in a normative population has not been adequately tested in patients with ET undergoing DBS.

We hypothesized that ET and healthy control participants differ in whole brain connectomes and that such differences manifest as somatomotor, thalamus, and cerebellum resting state network (RSN) differences. Furthermore, we hypothesized that pre-operative cerebellum-thalamus-somatomotor FC would predict tremor improvement after VIM DBS. We used rs-fMRI with stringent motion artifact reduction [22] and a combination of graph theoretical [23] and classical analytical techniques [24, 25] to identify patterns of aberrant FC in participants with medically refractory ET compared with age- and sex-matched healthy controls.

METHODS

PARTICIPANTS

Adults with a clinical diagnosis of ET [1] causing functional impairment despite optimized pharmacologic intervention (i.e., medically refractory) and scheduled for unilateral VIM DBS surgery were recruited from the Movement Disorders Center at Washington University (St. Louis, MO) between 2008–2017. Participants with other movement disorders, structural brain abnormalities, or major medical conditions were excluded. All ET patients provided informed consent for pre-operative MRI studies and the Washington University DBS Outcomes Project as approved by the Washington University Institutional Review Board (IRB), in agreement with the Declaration of Helsinki. Participants were instructed to continue to take medications as prescribed.

Healthy control data were obtained from rs-fMRI scans of healthy adults collected using the same imaging sequences and exclusion criteria under data sharing protocols approved by the Washington University IRB and in agreement with the Declaration of Helsinki [26, 27] on either of 2 MRI scanners of the same make and model and equipped with identical hardware and software. Healthy control data passing quality-assurance criteria (described below) were matched to the ET group by age, sex, and the proportion of scans conducted on each MRI scanner.

Tremor severity was assessed in participants with ET using the Fahn-Tolosa-Marin Tremor Rating Scale [28] parts A and B (TRS) pre-operatively and at their initial DBS programming visit (approximately one month post-operatively) in both the stimulation OFF state and again in the ON state after turning on the stimulators and completing initial programming. Response to DBS ($\Delta TRS_{OFF\text{-}ON}$) was measured as the absolute difference between OFF and ON TRS scores for the side contralateral to VIM DBS. Although DBS benefit

is incomplete immediately after initial programming, we adopted the current study design as medication changes confound long-term interpretation of DBS response and ON/OFF data were not consistently obtained after initial programming in our population.

DATA ACQUISITION

All participants underwent fMRI scans in a 3 Tesla TRIO scanner (Siemens AG) equipped with a standard 12-channel head coil. Participants completed up to a total of 22 minutes of resting state fMRI over 3 consecutive runs using a gradient echo pulse sequence [200 volumes/run, TR = 2200 ms, TE = 27 ms, 48 axial slices, FOV = 256 mm, flip angle = 90°, 4 mm^3 isotropic voxels]. Participants were instructed to close their eyes, remain still, and not fall asleep. Participants were directly observed for movement or signs of sleep during scanning and participants were asked about wakefulness at the completion of each run. Any runs during which participants were asleep or had sustained tremor were excluded. Anatomical imaging included one sagittal T1-weighted magnetization-prepared rapid gradient echo (MP-RAGE) scan (T1W) [TE = 3.14 ms, TR = 2400 ms, TI = 1000 ms, flip angle = 8˚, 0.9 mm^3 isotropic voxels] and one T2-weighted 3D scan (T2W) [TE = 461 ms, TR = 3200 ms, 0.9 mm^3 isotropic voxels].

PREPROCESSING

rs-fMRI data were preprocessed using standard techniques [29]: 1) atlas transformation via composition of affine transforms involving a sequence of co-registrations between the fMRI volumes, T2W and T1W structural images, and Talairach atlas target space; 2) realignment of images to correct for head motion; 3) regression of the voxel-wise mean signal and linear trend; 4) regression of several nuisance variables (motion regression derived by Volterra expansion [30] and signal from: ventricles, white matter and averaged over the whole brain); 5) generation of temporal masks flagging frames contaminated by excess motion (see *Motion Correction and Quality Assurance* below); 6) repeat removal of the voxel-wise mean signal and linear trend and regression of nuisance variables ignoring frames previously censored for motion; 7) linear interpolation to replace censored frames using least-squares spectral estimation (only used for band-pass filtering); 8) temporal band-pass filtering (0.009 Hz < f < 0.08 Hz) of the continuous, interpolated data; and 9) spatial smoothing (6 mm FWHM Gaussian blur in each cardinal direction).

To minimize group-specific atlas registration bias, we generated an atlas representative template from study-derived MP-RAGE data from an equal sampling of ET and healthy control participants [31]. Individual participant data were transformed to atlas space by composition of affine transforms involving a sequence of registrations between the fMRI volumes, T2W and T1W structural images, and the atlas template.

Anatomical T1-weighted images were processed using the FreeSurfer 5.0 default recon-all processing pipeline with manual edits. In brief, the FreeSurfer pipeline includes brain extraction, subcortical segmentation, intensity normalization, topology correction, surface deformation following intensity gradients to define boundaries between white matter, gray matter and cerebrospinal fluid, inflation of the surfaces to a sphere, registration to a spherical atlas, and parcellation of the cerebral cortex [32].

MOTION CORRECTION AND QUALITY ASSURANCE

Motion-related artifact is a major methodological and scientific issue in rs-fMRI research [33]. We applied rigorous quality assurance measures to minimize the impact of motion artifacts and movement confounds, including strict criteria for head motion. Framewise displacement was calculated from low-pass filtered [34] (fc = 0.1 Hz) motion parameters; volumes with filtered framewise displacement exceeding 0.1 mm were excluded [35]. After frame censoring, participants with fewer than 120 included fMRI volumes (i.e., 4.4 minutes of low motion data) were excluded. Preprocessing was then repeated using the updated temporal masks to remove volumes contaminated by motion from the outset of preprocessing.

STATISTICAL METHODS

Inter-group comparisons were performed for each baseline measure using an independent-samples *t*-test for continuous or chi-square test for categorical variables.

WHOLE BRAIN OBJECT-ORIENTED ANALYSES

We employed an unbiased approach to assess functional connectivity across the entire brain. Each brain was seeded with a set of 300 spherical seeds, including 239 × 10-mm diameter cortical- and 61 × 8-mm diameter subcortical and cerebellar seeds, providing whole-brain coverage [36], as validated and applied to the studies of Parkinson disease and dystonia [26, 27]. Seeds in the cerebral cortex, thalamus, and basal ganglia were assigned to 16 resting state networks following a previously published scheme [27]. Time courses were averaged across all included voxels for each seed and Pearson correlations were computed for each seed pair to create individual subject whole-brain correlation matrices. Correlation values were averaged across participants to obtain group-mean correlation

matrices. Group difference matrices were derived from subtraction of Fisher-z transformed group-mean data (control minus ET).

We employed a data-driven approach to identify large-scale group-level differences in resting-state functional connectivity using weighted object-oriented data analysis (OODA) [23]. Most functional neuroimaging studies suffer from the so-called *curse of dimensionality* [37] or '*small n, large p*' problem [38, 39] due to the large number of predictor variables (voxels) in fMRI and relatively small number of participants. OODA circumvents these challenges by directly comparing whole-brain connectivity matrices as objects [23]. OODA employs the parametric Gibbs distribution model to whole brain correlation matrices. We determined the central tendencies of each group (g*) matrix under the Gibbs distribution for each group, healthy control and ET, and the Euclidean distance between the healthy control- and ET central g* matrices. To assess statistical significance, we generated a distribution of distances by bootstrapping samples from each dataset (N = 1,000) to generate new central g* matrices as described by Gratton et al [27].

We used multidimensional scaling (MDS) to visually represent the dimensional distribution of individual correlation matrices based on the distances (i.e., dissimilarities) between them [23]. Euclidean distances between each pair of correlation matrices were calculated to generate a pairwise distance matrix. The matrix objects are then represented in a dimensional space where the principal components of distance are the primary dimensions. Each dot on the plot represents an individual correlation matrix and the distance between points correlates with their actual distance. The central tendencies of each group (g*) were also represented in the MDS plots. MDS computations were performed using the cmdscale.m function in MATLAB R2018b.

POST-HOC NETWORK ANALYSES

Following determination of significant whole brain matrix-level FC differences, we examined network-level FC between canonical RSNs to identify matrix-level differences. We calculated composite within- and between-network FC by taking the average pairwise correlation between unique network nodes to generate "block-average" network FC matrices [39, 40]. We selected six cross-network FC blocks *a priori* for hypothesis testing: thalamus-dorsal somatomotor, thalamus-lateral somatomotor, and thalamus-cerebellum based on previous work implicating these regions in the pathophysiology of ET; thalamus-visual, visual-lateral somatomotor, and visual-auditory were additionally tested based on the prominence of visual network findings in the OODA analysis and work suggesting relevance of visual networks in ET [11, 18–21].

Independent-samples *t*-tests assessed group-level differences in network FC. We corrected for multiple comparisons with a false discovery rate (FDR) of 10% to determine the significance threshold. FDR was selected because it explicitly informs about the maximum percentage of false positive and is a more powerful approach than family-wise type I error correction results [41]. For analyses in which the consequences of a false positive finding are relatively benign, a 5% FDR is too conservative and a 10–20% FDR is considered appropriate [42].

We examined medication effects in network-to-network blocks that significantly differed between ET and healthy control groups. We stratified ET participants by whether they were taking propranolol or primidone, the two most common medications in this cohort and applied a non-parametric Mann-Whitney-U test to determine whether either medication was associated with differences in FC. Other medications could not be assessed as they were taken by fewer than five participants.

REGRESSION OF NETWORK-LEVEL FC WITH CLINICAL MEASURES

To determine rs-fMRI markers of clinical relevance, we calculated a multiple linear regression to predict *a priori* network FC values based on tremor response (ΔTRS_{OFF-ON}), medication status for drugs with significant effects on network FC in this study (primidone), and the scanner used for data collection in ET participants. The visual-lateral somatomotor and thalamus-visual networks were chosen based on the combination of our network-level findings and prior reports of thalamo-visual-motor FC as a preoperative predictor of tremor arrest after VIM thalamotomy [18–21]. The cerebellar-thalamus and thalamus-lateral somatomotor networks were chosen based on literature implicating cerebello-thalamo-motor FC in the pathophysiology of tremor [4, 43, 44]. Significance thresholds were Bonferroni corrected for multiple comparisons. Significance was defined as $p < 0.025$.

REGIONAL ANALYSES

To further explore the spatial extent of the thalamic motor network in ET, we used a hypothesis-driven, seed-based approach to study motor thalamus FC across the entire brain [4]. We combined the four thalamus seeds assigned to the dorsal somatomotor network [36] into one bilateral motor thalamus seed containing the ventral intermediate nucleus (VIM), the principal cerebellar outflow target and our cohort's target for deep brain stimulation in essential tremor.

For each participant, time series data were extracted from each voxel within the seed and averaged over all included voxels. White matter and ventricular signals were masked from the seed image. Correlation maps were computed between each seed and all voxels in the brain using the Pearson product moment formula. Maps were transformed using Fisher z-transform to obtain z(r) maps that were averaged over participants to obtain group-mean correlation maps and group difference (control minus ET) z(r) images. To assess statistical significance, random effects analyses (voxel-wise t-map) were done at the group level and t-images were converted to equally probable Z-images and assessed for the presence of significant voxel clusters. Cluster-wise significance criteria were determined by non-parametric analysis of surrogate Z-images generated by Monte-Carlo permutation (10,000 iterations) simulation of the null hypothesis and corrected for multiple comparisons with a fixed false-positive rate of 5% [45].

RESULTS

PARTICIPANTS

We recruited 40 participants with ET and identified a like number of sex- and age-matched healthy controls. 13 participants were excluded prior to analysis (2 had comorbid neuropsychiatric diagnoses, 5 had observed rest tremor throughout scanning, and 2 had anatomic abnormalities on structural MRI). After application of rigorous quality assurance criteria, 21 participants with ET and 34 age/sex matched healthy control participants remained. All ET participants had bilateral upper limb tremor and subsequently underwent unilateral VIM DBS targeting the limb in which tremor caused more functional impairment (4 R VIM, 17 L VIM). Electrode placement in the VIM was visually localized and confirmed by post-operative CT scan co-registered to pre-operative MRI. Table 1 provides detailed demographic and clinical information for analyzed ET participants. Groups did not differ in demographic, MRI scanner, or fMRI motion parameters (Table 2).

ET WAS CHARACTERIZED BY DIFFERENCES IN THE WHOLE-BRAIN FUNCTIONAL CORRELATION MATRIX

Group-average correlation matrices for both the healthy controls and the ET participants showed typical network-related block structure characterized by high within-network FC (on diagonal blocks) and weakly positive or anti-correlated between-network FC (off-diagonal blocks) [36, 46] (Figure 1). We computed each group's central matrix object (g*) (essentially the group average correlation matrix) and their difference (HCl g* - ET g*) (Figure 2). This difference, taken as a whole, was statistically significant ($p = 0.048$). Post-hoc network level FC analyses revealed statistically significant effects involving the thalamus, somatomotor, visual, and auditory networks. Specifically, participants with ET showed less negative (i.e., weaker) dorsal somatomotor, lateral somatomotor and visual network correlations with the thalamus. Similarly, auditory and inferior somatomotor cortices showed less positive (i.e., weaker) correlations with visual areas (Figure 1C). Network-level FC block-average matrices are illustrated in the upper triangles of Figure 2. The Benjamini-Hochberg-corrected significance threshold (FDR 10%) was $p <= 0.040$.

ALTERED THALAMIC AND VISUAL-AUDITORY NETWORK-LEVEL FC IN ET

For the six *a priori* inter-network FC blocks, the ET group had significantly different FC between thalamus-lateral somatomotor, thalamus-dorsal somatomotor, thalamus-visual, and visual-auditory networks compared with healthy controls (Table 3). ET and healthy control groups did not differ in visual-lateral somatomotor or thalamus-cerebellum FC.

PRIMIDONE AFFECTS THALAMIC-LATERAL SOMATOMOTOR NETWORK FC

Primidone use in the ET group was associated with increased thalamus-lateral somatomotor network-level FC (*Mdn:* taking = 0.08, not taking = –0.03, U = 22, p = 0.02), but not thalamus-dorsal somatomotor, thalamus-visual, or visual-auditory FC. Propranolol had no systematic effect on FC in any of the tested networks (Figure 3).

ALTERED A PRIORI SEED-BASED THALAMIC REGIONAL FC

Both healthy control and ET groups had similar patterns of bilateral motor thalamus seed-based regional FC (Figure 4A-B). ET and healthy control motor thalamus regional FC patterns significantly differed in three clusters (Figure 4C): 1) right sensorimotor cortex, 2) bilateral occipitoparietal lobes, and 3) cerebellum (decreased in ET, highest level of significance $t \geq 2.0$). Table 3 summarizes significant seed-cluster results.

VISUAL-LATERAL SOMATOMOTOR NETWORK FC CORRELATES WITH TREMOR IMPROVEMENT FROM DBS

We calculated multiple linear regressions to predict visual-lateral somatomotor FC, thalamus-somatomotor FC, cerebellum-thalamus FC, and thalamus-visual FC based on $\Delta TRS_{OFF\text{-}ON}$, primidone status, and the MRI scanner on which data were collected. Results of the multiple linear

PARTICIPANT[a]	AGE (YEARS)	SEX	FAMILY HISTORY	DURATION (YEARS)	TRS[b]	$\Delta TRS_{(OFF-ON)}$ [b]	DOMINANT HAND	TREMOR MEDICATIONS (TOTAL DAILY DOSE IN MG)	INITIAL STIMULATION PARAMETERS				
									SITE	CONTACTS	V	PW	FREQ
ET1	66	F	sporadic	41	22	0	Right	propranolol 120, primidone 500, gabapentin 1800	L VIM	C+2-	1.0 V	60 μs	185 Hz
ET2	80	F	familial	12	44	2.5	Right	propranolol 140, primidone 750, gabapentin 300	L VIM	0–3+	2.3 V	60 μs	185 Hz
ET3	69	M	familial	41	41	8	Right	primidone 500, clonazepam 1.5	L VIM	C+0-	2.6 V	60 μs	185 Hz
ET4	77	M	familial	47	21	6	Right	primidone 350, metoprolol 25	L VIM	0–3+	2.5 V	60 μs	185 Hz
ET5	65	M	sporadic	55	36	2.5	Right	primidone 750	L VIM	C+1-	1.5 V	60 μs	185 Hz
ET6	58	F	sporadic	12	59	5.5	Right	propranolol 40, gabapentin 300	L VIM	C+2-	3.0 V	60 μs	185 Hz
ET7	62	M	familial	47	21	1	Right	propranolol 80	L VIM	C+2-	1.5 V	60 μs	185 Hz
ET8	55	M	familial	30	20	1	Right	clonazepam 3, carbidopa-levodopa 100/400	L VIM	1–3+	2.8 V	60 μs	185 Hz
ET9	48	M	sporadic	18	29	2	Left	propranolol 320, primidone 600	R VIM	1–3+	2.5 V	60 μs	185 Hz
ET10	81	M	familial	41	31	3	Right	propranolol 80	L VIM	1–3+	2.5 V	60 μs	185 Hz
ET11	62	M	sporadic	12	14	1	Right	none	L VIM	C+2-	2.0 V	60 μs	185 Hz
ET12	55	M	sporadic	10	27	5	Right	diazepam 30, zolpidem 10	R VIM	0+3-	2.0 V	60 μs	185 Hz
ET13	56	M	familial	2[c]	23	5	Right	propranolol 200, primidone 750	L VIM	1–3+	2.0 V	60 μs	185 Hz
ET14	52	F	sporadic	38	38	3	Right	carbidopa/levodopa 75/300	L VIM	0–3+	2.0 V	60 μs	185 Hz
ET15	49	F	sporadic	11	20	3.5	Right	clonazepam 1, carbidopa-levodopa 150/600	R VIM	1–3+	1.6 V	60 μs	185 Hz
ET16	66	M	familial	6	15	2.5	Right	none	L VIM	0–3+	1.3 V	60 μs	185 Hz
ET17	75	F	sporadic	35	18	2	Right	topiramate 200, primidone 500	L VIM	0+3-	2.0 V	60 μs	185 Hz
ET18	62	F	familial	10	30	2	Right	topiramate 100, propranolol 160	L VIM	1–3+	2.0 V	60 μs	185 Hz
ET19	76	M	familial	36	26	2	Right	propranolol 180, primidone 400	L VIM	C+1–3+	1.5 V	60 μs	185 Hz
ET20	55	F	familial	52	30	2.5	Left	pramipexole 1	R VIM	C+0+2-	2.0 V	60 μs	185 Hz
ET21	57	M	familial	38	21	2	Right	topiramate 200, primidone 1000	L VIM	C+1-	1.8 V	60 μs	130 Hz

Table 1 Demographic information: participants analyzed with essential tremor.

[a]19 additional participants were excluded from final analyses (N = 5: observed movement throughout scanning, N = 2: comorbid neuropsychiatric diagnoses, N = 2: anatomic abnormalities on structural MRI, N = 8: did not meet motion quality assurance criteria, N = 2: to correct group imbalance of the MRI scanners used for data collection).

[b]TRS represents the total score while TRS_{Off-On} reflects only tremor scores for limbs contralateral to VIM surgery.

[c]Clinical follow-up confirmed diagnosis of ET (symptoms >3 years).

Abbreviations: V = Voltage, PW = Pulse Width; Freq = Frequency.

	ET (N = 21) MEAN (SD)	CONTROL (N = 34) MEAN (SD)	STATISTIC	*P* VALUE
Age in years [range]	63.1 (10.1) [48–81]	61.9 (8.0) [49–82]	$T = 0.5$	0.62
Sex	38% F, 62% M	38% F, 62% M	$\chi^2 = 0.00$	1.00
Scanner	43% S1, 57% S2	41% S1, 59% S2	$\chi^2 = 0.02$	0.90
Handedness	90% right-handed	88% right-handed	$\chi^2 = 0.07$	0.80
Root mean square framewise displacement (mm)	0.056 (0.008)	0.053 (0.008)	$T = 3.34$	0.17
Number of frames kept	408.0 (107.8)	446.0 (118.2)	$T = -1.19$	0.24
TRS [range]	27.9 (10.9) [14–59]			

Table 2 Group matching data: essential tremor and control.

regression indicated that there was a strong collective significant effect between $\Delta TRS_{OFF\text{-}ON}$, primidone status, MRI scanner, and visual-lateral somatomotor FC, (F(3, 17) = 6.05, p = .005, R2 = 0.52, R2adj = 0.43). The individual predictors were examined further and indicated that $\Delta TRS_{OFF\text{-}ON}$ (t = –2.482, p = .024) and primidone status (t = –3.311, p = .004) were significant predictors in the model, and MRI scanner (t = –1.049, p = .309) was a non-significant predictor in the model. There was a moderate collective non-significant effect between $\Delta TRS_{OFF\text{-}ON}$, primidone status, MRI scanner, and thalamus-somatomotor FC, (F(3, 17) = 2.78, p = .073, R2 = 0.33, R2adj = 0.21). $\Delta TRS_{OFF\text{-}ON}$, primidone status, and MRI scanner did not predict cerebellum-thalamus FC, (F(3, 17) = 1.02, p = .410, R2 = 0.15, R2adj = 0) nor thalamus-visual FC, (F(3, 17) = 0.69, p = .569, R2 = 0.11, R2adj = –0.05). The regression model did not include propranolol status as it did not have a significant effect on any of the tested networks.

DISCUSSION

This study demonstrates whole-brain, network, and regional-level FC dysfunction in people with medically refractory ET and identifies visual-lateral somatomotor FC as a potential biomarker to predict tremor improvement after VIM DBS. OODA characterized group differences in the whole-brain correlation matrix without requiring substantial dimensionality reduction. This permitted the unbiased interpretation of FC differences within the larger context of the entire brain correlation matrix followed by focused inspection of functional relationships between

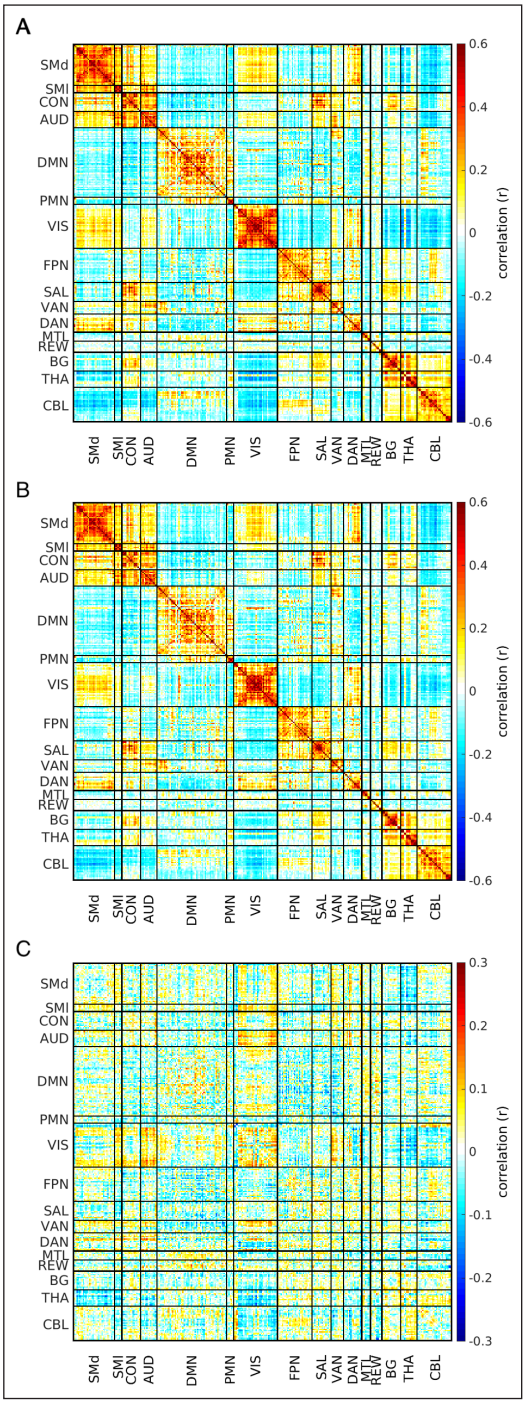


Figure 1 Group-level connectomes in ET and Controls. Large-scale functional connectomes in **(A)** Control and **(B)** ET participants reveal grossly similar resting state network organization, consistent with resting state network architecture found in other cohorts of healthy adults. Warm and cool colors indicate positive and negative correlations, respectively. **C:** A subtraction matrix (Control minus ET) shows selective network-to-network blocks of altered FC in ET, particularly involving thalamus and visual internetwork FC.

regions. The findings of our whole brain analysis support extant literature including altered cerebello-thalamo-cortical FC [47] and highlight the potential relevance of

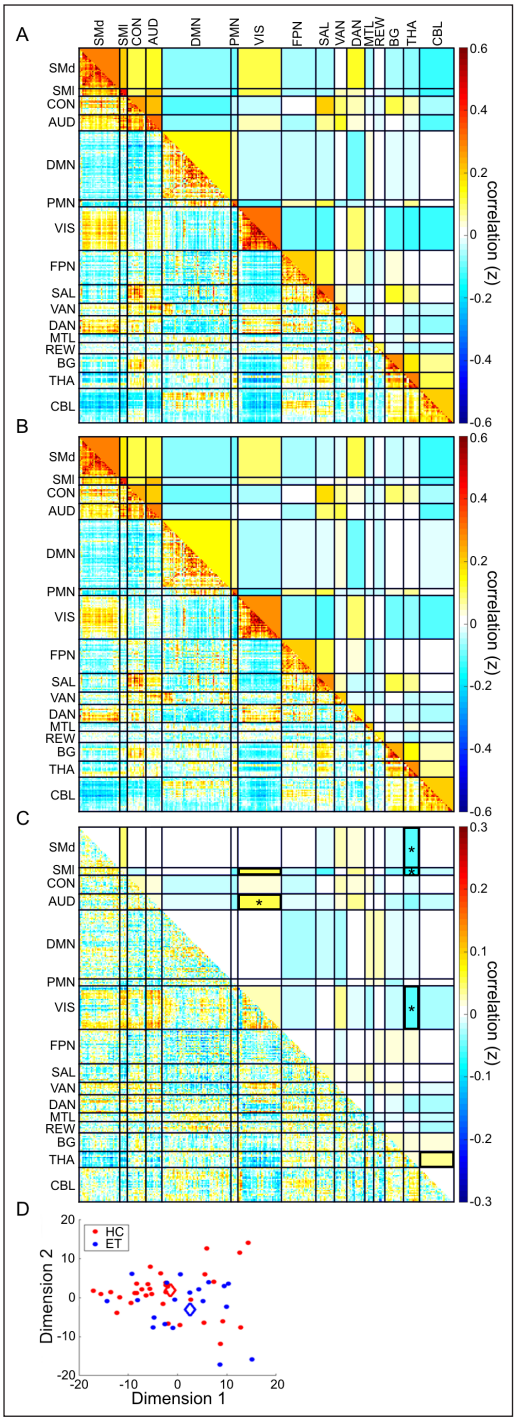


Figure 2 Disruption of large-scale network structure in ET. Central weighted connectome object (g*) for **(A)** Control and **(B)** ET groups and **(C)** subtraction (Control g* – ET g*). Upper triangles show composite block FC scores (average cross-correlation between seeds) while the lower triangles show the matrix objects with all edges preserved. Connectome objects differ significantly between ET and controls. Black outlines in the upper triangle indicate blocks chosen a priori for hypothesis testing of ET versus controls. Stars indicate blocks with significantly different network FC between ET and controls. Note the color scale difference in (C). **D:** Multidimensional scaling plot demonstrates separation of ET and control connectomes represented in 2-dimensional space. Diamonds indicate the central object for each group.

***A PRIORI* NETWORK**	**CONTROLS**	**ET**	**t-SCORE**	**p**
Thalamus – Lateral Somatomotor	–0.07	0.00	2.89	**< 0.01[a]**
Thalamus – Dorsal Somatomotor	–0.08	–0.03	2.50	**0.02[a]**
Thalamus – Visual	–0.13	–0.08	2.17	**< 0.04[a]**
Thalamus – Cerebellum	0.11	0.08	–1.70	0.09
Visual – Lateral Somatomotor	0.12	0.07	–1.66	0.10
Visual-Auditory	0.06	0.00	–2.54	**0.02[a]**
Significant Clusters	**ET compared to HC FC**	**t-score**	**cluster contiguous voxels**	
B. Motor Thalamus-Rt. sensorimotor cortex	(+)	**≥ 2.9***	113	
B. Motor Thalamus – B. occipitoparietal lobes	(–)	**≥ 4.0[a]**	8	
B. Motor Thalamus – Cerebellum	(–)	**≥ 2.0[a]**	1161	

Table 3 ET versus Health Control (HC) *a priori* network- (top) and regional- (bottom) functional connectivity (FC).

[a] Significant results.

other networks in the pathophysiology of ET. We identified robust differences in visual network FC. Furthermore, tremor improvement after VIM DBS is a significant negative predictor of visual-lateral somatomotor FC.

Abnormal thalamic FC is among the most consistent finding across functional neuroimaging studies of ET [4, 48–55]. We demonstrated increased average network-level FC between thalamus and somatomotor networks in ET.

Many neuroimaging studies show cerebellar involvement with ET, although the nature and location of these findings vary [56–58]. Electrophysiology and lesion studies provide strong evidence connecting action tremor to the cerebellum [59, 60]. Some pathology studies report cerebellar degeneration as evidenced by a loss of Purkinje cells, their connections, and atrophy in ET [61, 62], but the role of cerebellar pathological changes in ET is controversial [63].

We did not find abnormal cerebellum FC at the network level in ET, but we did identify decreased regional FC between bilateral motor thalamus and broad regions of the cerebellum. Several possibilities may account for this discrepancy. Our cerebellum network of 27 functionally-

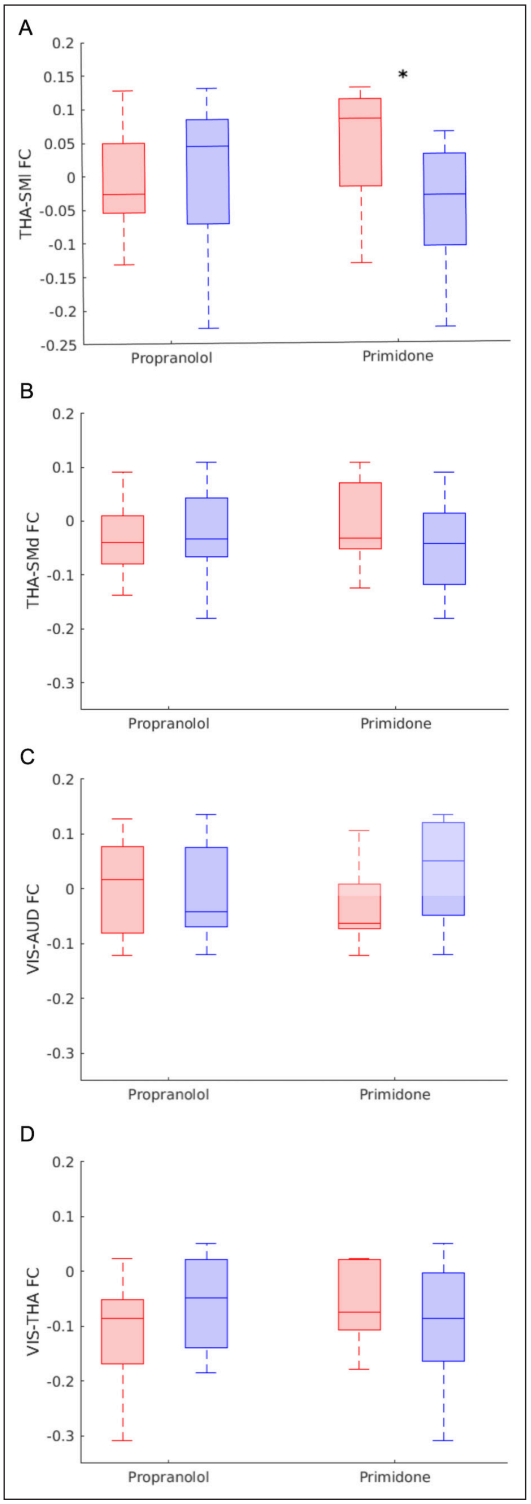


Figure 3 Medication effects on network FC. Composite FC scores for (clockwise from top left) thalamus-lateral somatomotor, visual-auditory, thalamus-dorsal somatomotor, and visual-thalamus networks in ET participants taking (red) and not taking (blue) propranolol (*N*: taking = 9, not taking = 12) or primidone (*N*: taking = 10, not taking = 11) at the time of MRI. The central line within each box indicates median FC. The bottom and top edges of the box represent the 25th and 75th percentiles, respectively. The whiskers indicate the minimum and maximum FC values within each group. *P < 0.05, uncorrected.

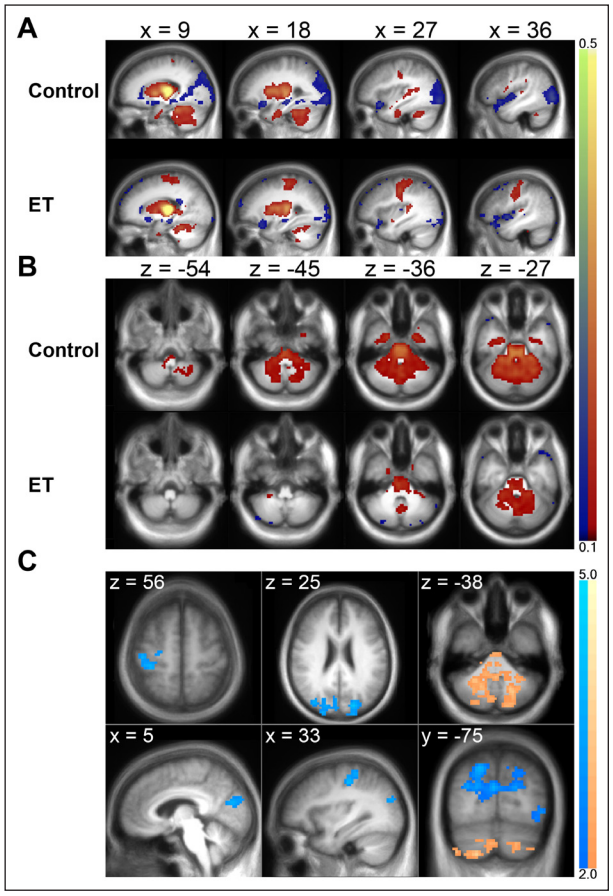


Figure 4 Bilateral motor thalamus FC in ET and controls. A-B: ET and control group average correlation maps for a bilateral motor thalamus seed are depicted in the (A) sagittal and (B) axial planes. In both groups, motor thalamus has positive FC with sensorimotor areas, cerebellum, and the whole thalamus and negative FC with occipitoparietal and superior temporal lobes. Color maps are thresholded at $|z| \geq 0.1$. Warm colors represent positive and cool colors represent negative correlations. **C:** Clusters of significant group difference are shown for the group effect z-score subtraction map (control minus ET) in the axial, coronal, and sagittal planes. The ET group has significantly increased FC with right sensorimotor cortex and decreased FC with occipitoparietal lobes, depicted in the first two columns. Note, ET has an increased magnitude of positive FC with sensorimotor cortex and decreased magnitude of negative FC with occipitoparietal cortex, both of which appear as net negative values in the difference map. The cerebellum has decreased FC in ET, shown in the rightmost column.

defined seeds provides broad coverage of the cerebellum but does not sample areas of potential importance to the pathophysiology of ET such as the deep cerebellar nuclei. Furthermore, we may not have detected a small magnitude network-level difference with our relatively small sample of 21 participants with ET. Finally, regional FC differences do not necessarily translate into altered network-level FC which are highly robust and stable [64]. Thus, differences in the cerebellum resting state networks may not be sensitive to focal cerebellar pathophysiology.

Visual inter-network FC differences featured prominently in our study. Neither primidone nor propranolol related to group-level differences in thalamus-visual FC, suggesting medications did not drive this effect. The role of visual networks in the pathophysiology and therapeutic mechanisms of ET have been increasingly recognized. ET is associated with abnormal visual network FC [47, 12, 65], where increased visual feedback exacerbates ET's tremor and relates to fMRI signal changes in cerebello-thalamo-motor, visual, and parietal areas [66]. Interestingly, removal of visual feedback attenuates intention tremor [67]. Although visual cortical regions are not generally recognized as involved in the pathogenesis of ET, our findings add to the growing body of work suggesting that visual-motor and visual-thalamic FC may relate to tremor reduction after thalamic surgeries [18–21]. Asynchrony between motor and visual systems may explain a visually-responsive action tremor with associated functional abnormalities in motor, subcortical, and visual networks. Discrepancies in visual feedback and motor system timings could plausibly induce periodic and aberrant movement "corrections." We demonstrate that visual-lateral somatomotor network FC is negatively associated with both tremor improvement after VIM DBS (i.e. weaker FC is associated with a stronger VIM DBS treatment response) and primidone status. This suggests that this network may reflect a shared therapeutic mechanism between different treatment modalities.

Although clinicians characterize ET as a pure motor disorder, patients have subtle impairments compared with age-matched healthy controls in complex visual and auditory attention and visuospatial function [68]. Abnormalities in visual network FC may also reflect these deficits. Prominent differences in visual internetwork FC are also observed in sleep versus awake conditions. In comparison to wake, drowsiness and non-rapid eye movement (NREM) sleep markedly increase the amplitude of spontaneous BOLD activity [69, 70], particularly in primary sensory and motor cortices [71–75]. This effect manifests as enhanced resting state functional connectivity (FC) within and between somatomotor and visual areas. Similarly, arousal fluctuations in nominally awake participants cause FC variability to be focally increased in these same areas [76]. Impaired sleep is not an established feature of essential tremor, however persons with essential tremor report higher levels of daytime sleepiness, possibly related to medication side effects [77]. Differences in arousal level may contribute to our findings, however we asked participants about level of wakefulness after each resting-state fMRI run and excluded those in which participants self-reported drowsiness or sleep. The similarities between our data and sleep-wake effects may be spurious given that sleep is grossly normal in essential tremor [78], and we also did not observe group differences in visual-motor FC that are expected with differences in arousal level [79, 80]. Furthermore, the magnitude of visual-somatomotor network FC was decreased in ET compared to controls, which is opposite of what would be expected if sedating medications or increased drowsiness were driving FC differences. Alternatively, the similarities may reflect common mechanisms involving the visual sensory network.

Resting-state networks are highly stable and conserved across individuals, arousal states, and even mammalian species [79–81]. Our findings of altered whole-brain and network- level FC in ET stand in contrast to similar analyses in focal dystonia in which only regional FC is altered while whole-brain and network-level FC are preserved despite the greater sample size and statistical power in the focal dystonia study [26, 27]. These data suggest that in comparison to focal dystonia, abnormalities in ET are more widespread across the brain and/or involve comparatively more network hub regions.

Our study design had several important limitations. First, participants were taking medications at the time of scanning, although these medications were not altered at the time of measured DBS response. Primidone related to increased FC between thalamus and lateral somatomotor networks, however prior work in medication-naïve individuals with ET has also shown increased thalamus-somatomotor FC [58], suggesting medication effects do not fully account for the differences in thalamo-cortical FC observed in this study. Though propranolol did not significantly relate to FC in any of the networks tested, this does not rule out that it may have a modest impact on FC which our study was not powered to detect. Larger studies are necessary to clarify how tremor-suppressing medications impact functional connectivity. Another significant limitation is that DBS outcome measures were limited to the initial programming session when settings are not yet optimized. Unfortunately, subsequent programming sessions in the current cohort did not include OFF TRS assessments. Comparisons between pre-operative TRS and optimized ON TRS at these later sessions were confounded by the effects of time and medication changes (many participants were able to wean medication after DBS). As such, the initial programming OFF vs ON TRS scores were the best proxy of DBS response in our data, though ideally, future studies would assess tremor in OFF vs ON states during follow-up programming sessions. Our study also did not include collection of cognitive performance measures, limiting our ability to assess non-motor correlates of FC. Finally, the relatively small sample size and overrepresentation of males in our study limit its generalizability, particularly given the significant heterogeneity within ET [56].

Nevertheless, the rigorous quality control at each step of preprocessing and analysis and novel statistical methods allow characterization of the group correlation matrix in ET while minimizing confounds and artifacts related to motion. Our whole-brain approach using OODA builds upon published work using seed- and ICA-based approaches to demonstrate abnormal cortical and subcortical FC. Furthermore, we provide evidence for robust effects in visual-somatomotor FC. Overall, we found that ET relates to whole-brain, network, and regional-level FC differences localized within thalamus, somatomotor, and visual regions using an unbiased, whole-brain approach to rs-fMRI analysis and that pre-operative visual-lateral somatomotor FC may predict response to VIM DBS.

ACKNOWLEDGEMENTS

Thank you to Susan R. Criswell, MD and Morvarid Karimi, MD for contributing healthy control data used in this study. Thank you to Aaron Tanenbaum, Jon Koller, Hugh Flores, and Linda Hood for technical assistance without whom this work would not be possible. Thank you to research coordinators Johanna Hartlein, Phil Lintzenich, Thomas Belcher, and My Vu for assistance with data collection.

FUNDING INFORMATION

NIH TL1 TR000096, RO1 NS041509, RO1 NS075321, RO1 NS097437, R01 NS124789, Schmidt Foundation for Integrative Brain Research, UR Provost Multidisciplinary Award, Geoffrey Waasdorp Pediatric Neurology Fund, Wilbur Smith Pediatric Neurology Fund, Barnes Jewish Hospital Foundation (Elliot Stein Family Fund), Barnes Jewish Hospital Foundation (Clinical Translational Research Award), and the Barbara & Sam Murphy Fund.

MORRIS, AIMEE E. NIH TL1 TR000096 NIH 5UE5NS090978-10, Schmidt Foundation for Integrative Brain Research, UR Provost Multidisciplinary Award.

CAMPBELL, MEGHAN C. NIH (NS097437, NS097799, NS075321, R61 AT010753, AT010753-02S1, AG065214; U19-AG071754); MJ Fox Foundation & Alzheimer Association; Washington University in St. Louis McDonnell Center for Systems Neuroscience, Mallinckrodt Institute of Radiology, and Neuroimaging Labs Innovation Award.

SNYDER, ABRAHAM Z. P30NS098577.

PERLMUTTER, JOEL S. (NIH: NINDS, NIA, NCATS) NS075321, NS103957, NS107281, NS092865, NS097437, U54NS116025, NS041509, Barnes-Jewish Hospital Foundation (Elliot Stein Family Fund and Parkinson disease research fund), American Parkinson Disease Association (APDA) Advanced Research Center at Washington University, Greater St. Louis Chapter of the APDA, Paula and Rodger Riney Fund, Jo Oertli Fund and Grant Williams Fund, and the Richard & Mary Jane Miller Fund.

MINK, JONATHAN W. (NIH: NINDS, NEI, NICHD) U24NS107165, U01NS101946, R01EY030183, P50HD103536, Schmidt Foundation for Integrative Brain Research, UR Provost Multidisciplinary Award, University of Rochester Child Neurology Endowment, the Geoffrey Waasdorp Pediatric Neurology Fund, and the Wilbur Smith Pediatric Neurology Fund.

NORRIS, SCOTT A. NIH NINDS: NS124789, NS107281, NS103957, U54NS116025, Dysphonia International, Michael J. Fox Foundation, and the Dystonia Medical Research Foundation.

COMPETING INTERESTS

The authors have no competing interests to declare.

AUTHOR AFFILIATIONS

Aimee E. Morris, M.D., Ph.D. orcid.org/0000-0002-9034-0484
University of Rochester School of Medicine and Dentistry, Rochester, NY, USA; Department of Neurology, Washington University School of Medicine, St. Louis, MO, USA
Babatunde Adeyemo, B.S.
Department of Neurology, Washington University School of Medicine, St. Louis, MO, USA
Meghan C. Campbell, Ph.D. orcid.org/0000-0003-3030-9669
Department of Neurology, Washington University School of Medicine, St. Louis, MO, USA; Department of Radiology, Washington University School of Medicine, St. Louis, MO, USA
Abraham Z. Snyder, M.D., Ph.D. orcid.org/0000-0002-3379-9627
Department of Neurology, Washington University School of Medicine, St. Louis, MO, USA; Department of Radiology, Washington University School of Medicine, St. Louis, MO, USA
Joel S. Perlmutter M.D. orcid.org/0000-0003-3263-8917
Department of Neurology, Washington University School of Medicine, St. Louis, MO, USA; Department of Radiology, Washington University School of Medicine, St. Louis, MO, USA; Department of Anatomy and Neurobiology, Washington University School of Medicine, St. Louis, MO, USA; Department

of Physical Therapy, Washington University School of Medicine, St. Louis, MO, USA
Jonathan W. Mink, M.D., Ph.D. orcid.org/0000-0002-7867-3710
Pittsford, NY, USA
Scott A. Norris, M.D. orcid.org/0000-0002-3835-0976
Department of Neurology, Washington University School of Medicine, St. Louis, MO, USA; Department of Radiology, Washington University School of Medicine, St. Louis, MO, USA

REFERENCES

1. **Bhatia KP, Bain P, Bajaj N,** et al. Consensus Statement on the classification of tremors. from the task force on tremor of the International Parkinson and Movement Disorder Society. *Mov Disord*. 2018;33:75–87. DOI: https://doi.org/10.1002/mds.27121
2. **He S, West TO, Plazas FR,** et al. Cortico-thalamic tremor circuits and their associations with deep brain stimulation effects in essential tremor. *Brain*. 2025;148:2093–2107. DOI: https://doi.org/10.1093/brain/awae387
3. **Hershey T, Mink JW.** Using functional neuroimaging to study the brain's response to deep brain stimulation. *Neurology*. 2006;66:1142–1143. DOI: https://doi.org/10.1212/01.wnl.0000216425.34178.dd
4. **Fang W, Chen H, Wang H,** et al. Essential tremor is associated with disruption of functional connectivity in the ventral intermediate Nucleus—Motor Cortex—Cerebellum circuit. *Hum Brain Mapp*. 2016;37:165–78. DOI: https://doi.org/10.1002/hbm.23024
5. **Gallea C, Popa T, Garcia-Lorenzo D,** et al. Intrinsic signature of essential tremor in the cerebello-frontal network. *Brain*. 2015;138:2920–2933. DOI: https://doi.org/10.1093/brain/awv171
6. **Jenkins IH, Bain PG, Colebatch JG, Thompson PD, Findley LJ, Frackowiak RS, Marsden CD, Brooks DJ.** A positron emission tomography study of essential tremor: evidence for overactivity of cerebellar connections. *Ann Neurol*. 1993;34:82–90. DOI: https://doi.org/10.1002/ana.410340115
7. **Nicoletti V, Cecchi P, Pesaresi I, Frosini D, Cosottini M, Ceravolo R.** Cerebello-thalamo-cortical network is intrinsically altered in essential tremor: evidence from a resting state functional MRI study. *Sci Rep*. 2020;10:16661. DOI: https://doi.org/10.1038/s41598-020-73714-9
8. **Lee D, Gan S-R, Faust PL, Louis ED, Kuo S-H.** Climbing fiber-Purkinje cell synaptic pathology across essential tremor subtypes. *Parkinsonism Relat Disord*. 2018;51:24–29. DOI: https://doi.org/10.1016/j.parkreldis.2018.02.032
9. **Choe M, Cortés E, Vonsattel J-PG, Kuo S-H, Faust PL, Louis ED.** Purkinje cell loss in essential tremor: Random sampling quantification and nearest neighbor analysis. *Mov Disord*. 2016. DOI: https://doi.org/10.1002/mds.26490
10. **Louis E, Vonsattel J, Honig L, Ross G, Lyons K, Pahwa R.** Neuropathologic findings in essential tremor. *Neurology*. 2006;66:1756–1759. DOI: https://doi.org/10.1212/01.wnl.0000218162.80315.b9
11. **Archer DB, Coombes SA, Chu WT, Chung JW, Burciu RG, Okun MS, Wagle Shukla A, Vaillancourt DE.** A widespread visually-sensitive functional network relates to symptoms in essential tremor. *Brain*. 2018;141:472–485. DOI: https://doi.org/10.1093/brain/awx338
12. **Tuleasca C, Najdenovska E, Regis J,** et al. Pretherapeutic Motor Thalamus Resting-State Functional Connectivity with Visual Areas Predicts Tremor Arrest After Thalamotomy for Essential Tremor: Tracing the Cerebello-thalamo-visuo-motor Network. *World Neurosurg*. 2018;117:e438–449. DOI: https://doi.org/10.1016/j.wneu.2018.06.049
13. **Wang P, Luo X, Zhong C, Yang L, Guo F, Yu N.** Resting state fMRI reveals the altered synchronization of BOLD signals in essential tremor. *J Neurol Sci*. 2018;392:69–76. DOI: https://doi.org/10.1016/j.jns.2018.07.008
14. **Perlmutter JS, Mink JW.** Deep brain stimulation. *Annu Rev Neurosci*. 2006;29:229–57. DOI: https://doi.org/10.1146/annurev.neuro.29.051605.112824
15. **Perlmutter JS, Mink JW, Bastian AJ, Zackowski K, Hershey T, Miyawaki E, Koller W, Videen TO.** Blood flow responses to deep brain stimulation of thalamus. *Neurology*. 2002;58:1388–1394. DOI: https://doi.org/10.1212/WNL.58.9.1388
16. **Grimm F, Walcker M, Milosevic L, Naros G, Bender B, Weiss D, Gharabaghi A.** Strong connectivity to the sensorimotor cortex predicts clinical effectiveness of thalamic deep brain stimulation in essential tremor. *Neuroimage Clin*. 2024. https://doi.org/10.1016/J.NICL.2024.103709
17. **Middlebrooks EH, Okromelidze L, Wong JK,** et al. Connectivity correlates to predict essential tremor deep brain stimulation outcome: Evidence for a common treatment pathway. *Neuroimage Clin*. 2021;32:102846. DOI: https://doi.org/10.1016/j.nicl.2021.102846
18. **Tuleasca C, Najdenovska E, Régis J,** et al. Clinical response to Vim's thalamic stereotactic radiosurgery for essential tremor is associated with distinctive functional connectivity patterns. *Acta Neurochir* (Wien). 2018;160:611–624. DOI: https://doi.org/10.1007/s00701-017-3456-x
19. **Tuleasca C, Bolton T, Régis J, Najdenovska E, Witjas T, Girard N, Thiran J-P, Levivier M, Van De Ville D.** Thalamotomy for tremor normalizes aberrant pre-therapeutic visual cortex functional connectivity. *Brain*. 2019;142:e57. DOI: https://doi.org/10.1093/brain/awz299
20. **Tuleasca C, Bolton TAW, Régis J,** et al. Normalization of aberrant pretherapeutic dynamic functional connectivity of extrastriate visual system in patients who underwent thalamotomy with stereotactic radiosurgery for

essential tremor: a resting-state functional MRI study. *J Neurosurg*. 2019;132:1792–1801. DOI: https://doi.org/10.3171/2019.2.JNS183454

21. **Al-Fatly B, Ewert S, Kübler D, Kroneberg D, Horn A, Kühn AA.** Connectivity profile of thalamic deep brain stimulation to effectively treat essential tremor. *Brain*. 2019;142:3086–3098. DOI: https://doi.org/10.1093/brain/awz236
22. **Power JD, Schlaggar BL, Petersen SE.** Recent progress and outstanding issues in motion correction in resting state fMRI. *Neuroimage*. 2014;105:536–551. DOI: https://doi.org/10.1016/j.neuroimage.2014.10.044
23. **La Rosa PS, Brooks TL, Deych E, Shands B, Prior F, Larson-Prior LJ, Shannon WD.** Gibbs distribution for statistical analysis of graphical data with a sample application to fcMRI brain images. *Stat Med*. 2016;35:566–580. DOI: https://doi.org/10.1002/sim.6757
24. **Power JD, Cohen AL, Nelson SSM,** et al. Functional network organization of the human brain. *Neuron*. 2011;72:665–678. DOI: https://doi.org/10.1016/j.neuron.2011.09.006
25. **Fox MD, Raichle ME.** Spontaneous fluctuations in brain activity observed with functional magnetic resonance imaging. *Nat Rev Neurosci*. 2007;8:700–11. DOI: https://doi.org/10.1038/nrn2201
26. **Norris SA, Morris AE, Campbell MC, Karimi M, Adeyemo B, Paniello RC, Snyder AZ, Petersen SE, Mink JW, Perlmutter JS.** Regional, not global, functional connectivity contributes to isolated focal dystonia. *Neurology*. 2020;95:e2246–e2258. DOI: https://doi.org/10.1212/WNL.0000000000010791
27. **Gratton C, Koller JM, Shannon W, Greene DJ, Maiti B, Snyder AZ, Petersen SE, Perlmutter JS, Campbell MC.** Emergent Functional Network Effects in Parkinson Disease. *Cerebral Cortex*. 2018;bhy121. DOI: https://doi.org/10.1093/cercor/bhy121
28. **Fahn S, Tolosa E, Marin C.** Clinical rating scale for tremor. In: Jankovic J, Tolosa E, editors. *Parkinson's disease and movement disorders*. Baltimore: Williams and Wilkins; 1993. pp. 271–280.
29. **Miezin FM, Maccotta L, Ollinger JM, Petersen SE, Buckner RL.** Characterizing the hemodynamic response: effects of presentation rate, sampling procedure, and the possibility of ordering brain activity based on relative timing. *Neuroimage*. 2000;11:735–59. DOI: https://doi.org/10.1006/nimg.2000.0568
30. **Friston KJ, Williams S, Howard R, Frackowiak RS, Turner R.** Movement-related effects in fMRI time-series. *Magn Reson Med*. 1996;35:346–55. DOI: https://doi.org/10.1002/mrm.1910350312
31. **Buckner RL, Head D, Parker J, Fotenos AF, Marcus D, Morris JC, Snyder AZ.** A unified approach for morphometric and functional data analysis in young, old, and demented adults using automated atlas-based head size normalization: reliability and validation against manual measurement of total intracranial volume. *Neuroimage*. 2004;23:724–38. DOI: https://doi.org/10.1016/j.neuroimage.2004.06.018
32. **Fischl B.** FreeSurfer. *Neuroimage*. 2012;62:774–81. DOI: https://doi.org/10.1016/j.neuroimage.2012.01.021
33. **Power JD, Barnes KA, Snyder AZ, Schlaggar BL, Petersen SE.** Spurious but systematic correlations in functional connectivity MRI networks arise from subject motion. *Neuroimage*. 2012;59:2142–54. DOI: https://doi.org/10.1016/j.neuroimage.2011.10.018
34. **Gratton C, Dworetsky A, Coalson RS,** et al. Removal of high frequency contamination from motion estimates in single-band fMRI saves data without biasing functional connectivity. *Neuroimage*. 2020;217:116866. DOI: https://doi.org/10.1016/j.neuroimage.2020.116866
35. **Gratton C, Dworetsky A, Coalson RS,** et al. Removal of high frequency contamination from motion estimates in single-band fMRI saves data without biasing functional connectivity. *Neuroimage*. 2020;217:116866. DOI: https://doi.org/10.1016/j.neuroimage.2020.116866
36. **Seitzman BA, Gratton C, Marek S, Raut RV, Dosenbach NUF, Schlaggar BL, Petersen SE, Greene DJ.** A set of functionally-defined brain regions with improved representation of the subcortex and cerebellum. *Neuroimage*. 2020;206:116290. DOI: https://doi.org/10.1016/j.neuroimage.2019.116290
37. **Bellman RE.** *Adaptive Control Processes: A Guided Tour*; 1961. DOI: https://doi.org/10.1002/zamm.19620420718
38. **Fort G, Lambert-Lacroix S.** Classification using partial least squares with penalized logistic regression. *Bioinformatics*. 2005;21:1104–1111. DOI: https://doi.org/10.1093/bioinformatics/bti114
39. **Snyder AZ, Nishino T, Shimony JS,** et al. Covariance and Correlation Analysis of Resting State Functional Magnetic Resonance Imaging Data Acquired in a Clinical Trial of Mindfulness-Based Stress Reduction and Exercise in Older Individuals. *Front Neurosci*. 2022. https://doi.org/10.3389/fnins.2022.825547
40. **Brier MR, Thomas JB, Snyder AZ, Benzinger TL, Zhang D, Raichle ME, Holtzman DM, Morris JC, Ances BM.** Loss of intranetwork and internetwork resting state functional connections with Alzheimer's disease progression. *J Neurosci*. 2012;32:8890–9. DOI: https://doi.org/10.1523/JNEUROSCI.5698-11.2012
41. **Glickman ME, Rao SR, Schultz MR.** False discovery rate control is a recommended alternative to Bonferroni-type adjustments in health studies. *J Clin Epidemiol*. 2014;67:850–7. DOI: https://doi.org/10.1016/j.jclinepi.2014.03.012
42. **McDonald JH.** *Handbook of Biological Statistics*, 3rd ed. Sparky House Publishing; 2014.
43. **Lenka A, Bhalsing KS, Panda R, Jhunjhunwala K, Naduthota RM, Saini J, Bharath RD, Yadav R, Pal PK.** Role of altered

cerebello-thalamo-cortical network in the neurobiology of essential tremor. *Neuroradiology*. 2017;59:157–168. DOI: https://doi.org/10.1007/s00234-016-1771-1

44. **Nicoletti V, Cecchi P, Pesaresi I, Frosini D, Cosottini M, Ceravolo R.** Cerebello-thalamo-cortical network is intrinsically altered in essential tremor: evidence from a resting state functional MRI study. *Sci Rep*. 2020;10:16661. DOI: https://doi.org/10.1038/s41598-020-73714-9
45. **Eklund A, Nichols TE, Knutsson H.** Cluster failure: Why fMRI inferences for spatial extent have inflated false-positive rates. *Proceedings of the National Academy of Sciences*. 2016;113:7900–7905. DOI: https://doi.org/10.1073/pnas.1602413113
46. **Gotts SJ, Gilmore AW, Martin A.** Brain networks, dimensionality, and global signal averaging in resting-state fMRI: Hierarchical network structure results in low-dimensional spatiotemporal dynamics. *Neuroimage*. 2020;205:116289. DOI: https://doi.org/10.1016/j.neuroimage.2019.116289
47. **Lan H, Suo X, Li W,** et al. Abnormalities of intrinsic brain activity in essential tremor: A meta-analysis of resting-state functional imaging. *Hum Brain Mapp*. 2021;42:3156–3167. DOI: https://doi.org/10.1002/hbm.25425
48. **Wang P, Luo X, Zhong C, Yang L, Guo F, Yu N.** Resting state fMRI reveals the altered synchronization of BOLD signals in essential tremor. *J Neurol Sci*. 2018;392:69–76. DOI: https://doi.org/10.1016/j.jns.2018.07.008
49. **Mueller K, Jech R, Hoskovcová M, Ulmanová O, Urgošík D, Vymazal J, Růžička E.** General and selective brain connectivity alterations in essential tremor: A resting state fMRI study. *Neuroimage Clin*. 2017;16:468–476. DOI: https://doi.org/10.1016/j.nicl.2017.06.004
50. **Younger E, Ellis EG, Parsons N, Pantano P, Tommasin S, Caeyenberghs K, Benito-León J, Romero JP, Joutsa J, Corp DT.** Mapping Essential Tremor to a Common Brain Network Using Functional Connectivity Analysis. *Neurology*. 2023;101:e1483. DOI: https://doi.org/10.1212/WNL.0000000000207701
51. **Gallea C, Popa T, Garcia-Lorenzo D,** et al. Intrinsic signature of essential tremor in the cerebello-frontal network. *Brain*. 2015;138:2920–2933. DOI: https://doi.org/10.1093/brain/awv171
52. **DeSimone JC, Archer DB, Vaillancourt DE, Wagle Shukla A.** Network-level connectivity is a critical feature distinguishing dystonic tremor and essential tremor. *Brain*. 2019;awz085. DOI: https://doi.org/10.1093/brain/awz085
53. **Li J-Y, Suo X-L, Li N-N,** et al. Altered spontaneous brain activity in essential tremor with and without resting tremor: a resting-state fMRI study. *MAGMA*. 2021;34:201–212. DOI: https://doi.org/10.1007/s10334-020-00865-1
54. **Sharifi S, Buijink AWG, Luft F, Scheijbeler EP, Potters WV, van Wingen G, Heida T, Bour LJ, van Rootselaar AF.** Differences in Olivo-Cerebellar Circuit and Cerebellar Network Connectivity in Essential Tremor: a Resting State fMRI Study. *Cerebellum*. 2023;22:1123–1136. DOI: https://doi.org/10.1007/s12311-022-01486-1
55. **Buijink AWG, van der Stouwe AMM, Broersma M, Sharifi S, Groot PFC, Speelman JD, Maurits NM, van Rootselaar A-F.** Motor network disruption in essential tremor: a functional and effective connectivity study. *Brain*. 2015;138:2934–47. DOI: https://doi.org/10.1093/brain/awv225
56. **Mavroudis I, Petridis F, Kazis D.** Neuroimaging and neuropathological findings in essential tremor. *Acta Neurol Scand*. 2019;139:491–496. DOI: https://doi.org/10.1111/ane.13101
57. **Cerasa A, Quattrone A.** Linking Essential Tremor to the Cerebellum-Neuroimaging Evidence. *Cerebellum*. 2016;15:263–275. DOI: https://doi.org/10.1007/s12311-015-0739-8
58. **Fang W, Chen H, Wang H,** et al. Essential tremor is associated with disruption of functional connectivity in the ventral intermediate Nucleus—Motor Cortex—Cerebellum circuit. *Hum Brain Mapp*. 2016;37:165–78. DOI: https://doi.org/10.1002/hbm.23024
59. **Thach WT, Goodkin HP, Keating JG.** The cerebellum and the adaptive coordination of movement. *Annu Rev Neurosci*. 1992;15:403–42. DOI: https://doi.org/10.1146/annurev.ne.15.030192.002155
60. **Bosch TJ, Groth C, Espinoza AI, Bharmauria V, Flouty O, Singh A.** Cerebellar Oscillatory Patterns in Essential Tremor: Modulatory Effects of VIM-DBS. *The Cerebellum*. 2025;24:1–10. DOI: https://doi.org/10.1007/s12311-025-01787-1
61. **Lee A, Furuya S, Altenmüller E.** Epidemiology and treatment of 23 musicians with task specific tremor. *J Clin Mov Disord*. 2014;1:5. DOI: https://doi.org/10.1186/2054-7072-1-5
62. **Cameron E, Dyke JP, Hernandez N, Louis ED, Dydak U.** Cerebral gray matter volume losses in essential tremor: A case-control study using high resolution tissue probability maps. *Parkinsonism Relat Disord*. 2018;51:85–90. DOI: https://doi.org/10.1016/j.parkreldis.2018.03.008
63. **Rajput A, Robinson CA, Rajput AH.** Essential tremor course and disability: A clinicopathologic study of 20 cases. *Neurology*. 2004;62:932–936. DOI: https://doi.org/10.1212/01.WNL.0000115145.18830.1A
64. **Damoiseaux JS, Rombouts SARB, Barkhof F, Scheltens P, Stam CJ, Smith SM, Beckmann CF.** Consistent resting-state networks across healthy subjects. *Proceedings of the National Academy of Sciences*. 2006;103:13848–13853. DOI: https://doi.org/10.1073/pnas.0601417103
65. **Benito-León J, Sanz-Morales E, Melero H, Louis ED, Romero JP, Rocon E, Malpica N.** Graph theory analysis of resting-state functional magnetic resonance imaging in essential tremor. *Hum Brain Mapp*. 2019;40:4686–4702. DOI: https://doi.org/10.1002/hbm.24730
66. **Archer DB, Coombes SA, Chu WT, Chung JW, Burciu RG, Okun MS, Wagle Shukla A, Vaillancourt DE.** A widespread

visually-sensitive functional network relates to symptoms in essential tremor. *Brain*. 2018;141:472–485. DOI: https://doi.org/10.1093/brain/awx338

67. **Feys P, Helsen WF, Liu X, Lavrysen A, Loontjens V, Nuttin B, Ketelaer P.** Effect of visual information on step-tracking movements in patients with intention tremor due to multiple sclerosis. *Mult Scler*. 2003;9:492–502. DOI: https://doi.org/10.1191/1352458503ms949oa
68. **Tröster AI, Woods SP, Fields JA, Lyons KE, Pahwa R, Higginson CI, Koller WC.** Neuropsychological deficits in essential tremor: an expression of cerebello-thalamo-cortical pathophysiology? *Eur J Neurol*. 2002;9:143–51. DOI: https://doi.org/10.1046/j.1468-1331.2002.00341.x
69. **Larson-Prior LJ, Zempel JM, Nolan TS, Prior FW, Snyder AZ, Raichle ME.** Cortical network functional connectivity in the descent to sleep. *Proc Natl Acad Sci U S A*. 2009;106:4489–94. DOI: https://doi.org/10.1073/pnas.0900924106
70. **Bijsterbosch J, Harrison S, Duff E, Alfaro-Almagro F, Woolrich M, Smith S.** Investigations into within- and between-subject resting-state amplitude variations. *Neuroimage*. 2017;159:57–69. DOI: https://doi.org/10.1016/j.neuroimage.2017.07.014
71. **Song C, Boly M, Tagliazucchi E, Laufs H, Tononi G.** fMRI spectral signatures of sleep. *Proc Natl Acad Sci U S A*. 2022. DOI: https://doi.org/10.1073/PNAS.2016732119
72. **Boly M, Perlbarg V, Marrelec G, Schabus M, Laureys S, Doyon J, Pélégrini-Issac M, Maquet P, Benali H.** Hierarchical clustering of brain activity during human nonrapid eye movement sleep. *Proc Natl Acad Sci U S A*. 2012;109:5856–5861. DOI: https://doi.org/10.1073/pnas.1111133109
73. **Tagliazucchi E, Laufs H.** Decoding wakefulness levels from typical fMRI resting-state data reveals reliable drifts between wakefulness and sleep. *Neuron*. 2014;82:695–708. DOI: https://doi.org/10.1016/j.neuron.2014.03.020
74. **Mitra A, Snyder AZ, Tagliazucchi E, Laufs H, Raichle ME.** Propagated infra-slow intrinsic brain activity reorganizes across wake and slow wave sleep. *Elife*. 2015;4:e10781. DOI: https://doi.org/10.7554/eLife.10781
75. **Tsai PJ, Chen SCJ, Hsu CY, Wu CW, Wu YC, Hung CS, Yang AC, Liu PY, Biswal B, Lin CP.** Local awakening: regional reorganizations of brain oscillations after sleep. *Neuroimage*. 2014;102 Pt 2:894–903. DOI: https://doi.org/10.1016/j.neuroimage.2014.07.032
76. **Laumann TO, Gordon EM, Adeyemo B,** et al. Functional System and Areal Organization of a Highly Sampled Individual Human Brain. *Neuron*. 2015;87:657–70. DOI: https://doi.org/10.1016/j.neuron.2015.06.037
77. **Gerbin M, Viner AS, Louis ED.** Sleep in essential tremor: a comparison with normal controls and Parkinson's disease patients. *Parkinsonism Relat Disord*. 2012;18: 279–84. DOI: https://doi.org/10.1016/j.parkreldis.2011.11.004
78. **Jiménez-Jiménez FJ, Alonso-Navarro H, García-Martín E, Agúndez JAG.** Sleep disorders in essential tremor: systematic review and meta-analysis. *Sleep*. 2020. https://doi.org/10.1093/sleep/zsaa039
79. **Laumann TO, Snyder AZ, Mitra A,** et al. On the Stability of BOLD fMRI Correlations. *Cereb Cortex*. 2017;27:4719–4732. DOI: https://doi.org/10.1093/cercor/bhw265
80. **Larson-Prior LJ, Zempel JM, Nolan TS, Prior FW, Snyder AZ, Raichle ME.** Cortical network functional connectivity in the descent to sleep. *Proc Natl Acad Sci U S A*. 2009;106:4489–94. DOI: https://doi.org/10.1073/pnas.0900924106
81. **Vincent JL, Patel GH, Fox MD, Snyder AZ, Baker JT, Van Essen DC, Zempel JM, Snyder LH, Corbetta M, Raichle ME.** Intrinsic functional architecture in the anaesthetized monkey brain. *Nature*. 2007;447:83–6. DOI: https://doi.org/10.1038/nature05758

TO CITE THIS ARTICLE:
Morris AE, Adeyemo B, Campbell MC, Snyder AZ, Perlmutter JS, Mink JW, Norris SA. Thalamic and Visual Network Dysfunction Relates to Tremor Response in Thalamic Deep Brain Stimulation. *Tremor and Other Hyperkinetic Movements*. 2025; 15(1): 34, pp. 1–15. DOI: https://doi.org/10.5334/tohm.1039

Submitted: 01 May 2025 **Accepted:** 16 June 2025 **Published:** 01 August 2025

COPYRIGHT:
© 2025 The Author(s). This is an open-access article distributed under the terms of the Creative Commons Attribution 4.0 International License (CC-BY 4.0), which permits unrestricted use, distribution, and reproduction in any medium, provided the original author and source are credited. See http://creativecommons.org/licenses/by/4.0/.

Tremor and Other Hyperkinetic Movements is a peer-reviewed open access journal published by Ubiquity Press.